

FIG. 3. Magnetization dependence on  $P/H$  for 0.02 porosity YIG. The pressure variation is from 0.2 to 4 kbar.  $\blacktriangle$  and  $\blacksquare$  correspond to 8 and 16 Oe, respectively.

(i) There is initial quadratic behavior in extreme saturation as was expected from the series solution in Eq. (11).

(ii) There is subsequent linear behavior down to almost  $\frac{9}{10}$  saturation as expected from Eq. (13).

(iii) The slope in the linear region normalized by the porosity is independent of porosity, in accordance with Eq. (13). A value of  $\gamma=0.21$ , the constant in Eq. (13), is obtained from each curve in Fig. 2.

(iv) For still lower magnetization the solution deviates from linearity and is asymptotic to  $\frac{1}{4}\pi$ . This is a consequence of the chosen model but is physically realistic in that this would be the region where cavities would begin to interact and saturation effects would occur.

#### V. EXPERIMENTAL COMPARISON

Although the work of Wayne *et al.*<sup>6</sup> suggested this calculation, their data are not well suited for comparison with these theoretical results for the following reasons. First, many of their data are not in the approach to the saturation region. Secondly, they tabulated  $M(P)/M(0)$  rather than  $M(P)/M_s$  for various values of  $P$  and  $H$ . The difference, however, is probably due to crystal anisotropy effects which have not been considered in this calculation in order to emphasize the induced strain contribution. Since these are the only data available, this difficulty was ignored and experimental comparison was made which strongly supports the calculation, subject to this limitation. The following comparisons were made:

(i) The data were plotted as a function of  $P/H$ . This was found to be a good variable.

(ii) The behavior of YIG was the most carefully considered in Ref. 6. The magnetization curve for YIG was observed to have an initial quadratic

behavior followed by linear behavior as is seen in Fig. 3.

(iii) Slopes in the linear region for the three materials considered (see Figs. 4–6) were obtained and normalized for material properties. The values obtained were  $\gamma=0.16$ , 0.24, and 0.26, respectively, for YIG, manganese-zinc ferrite, and nickel ferrite. This is to be compared with a value of 0.21 obtained from the numerical solution. This agreement is encouraging since the material properties and porosities of the three ferrites considered are quite varied.

#### VI. DISCUSSION

A careful analysis of the calculation presented in Secs. II–IV reveals that the linear behavior over a

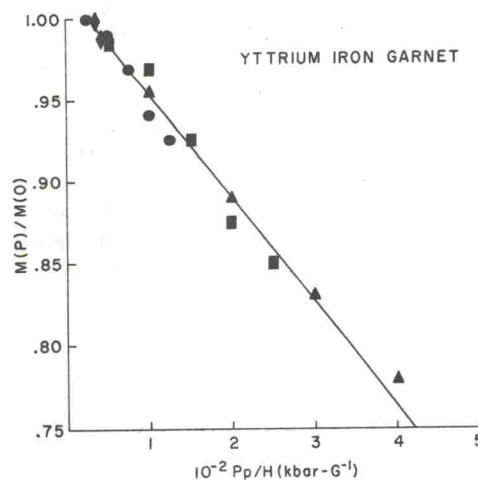


FIG. 4. Magnetization dependence on  $Pp/H$  for 0.02 porosity YIG. The pressure variation is from 2 to 20 kbar.  $\blacktriangle$ ,  $\blacksquare$ ,  $\bullet$ , and  $\blacklozenge$  correspond to external applied fields of 8, 16, 39, and 89 Oe, respectively.

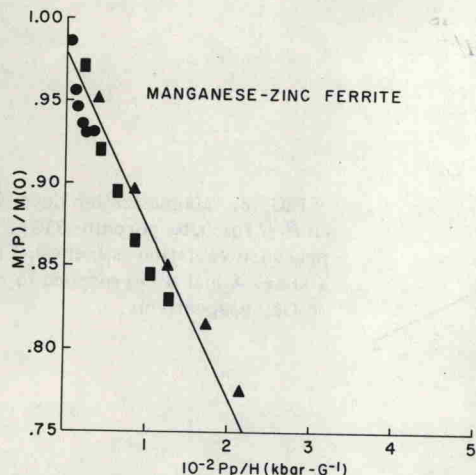


FIG. 5. Magnetization for 0.075 porosity  $\text{Mn}_{0.62}\text{Zn}_{0.25}\text{Fe}_{2.13}\text{O}_4$ . The pressure variation is from 2 to 12 kbar.  $\blacktriangle$ ,  $\blacksquare$ , and  $\bullet$  correspond to external applied fields of 35, 70, and 290 Oe, respectively.

limited region of the  $1/H$  axis (see Fig. 2) is a consequence of the  $1/r^3$  dependence of the strain field in Eq. (4). This is shown in the Appendix. Since the primary goal is to suggest that this calculation is relevant to magnetic material where there is no external pressure but where there is inherent internal strain, some discussion of the form of this internal strain is necessary. In real material there are many defects around which internal strain will occur. Cavities, inclusions, microcracks, dislocations, impurities, vacancies, interstitial atoms, and grain boundaries will all contribute. Relevance of the present calculation to cases in which internal strain is present assumes that a significant portion of the internal strain falls off as  $1/r^3$  from the defect around which it originates. Although the sources of internal strain are not completely understood, several examples may add credibility to this assumption.

(a) A source of internal strain occurs when a material is cooled from some elevated temperature to room temperature. For instance, consider a spherical inclusion of radius  $a$  with a thermal expansion coefficient smaller than the surrounding medium. Thermal contraction will create a pressure  $P_i$  within this inclusion. The strain field induced in the material surrounding the inclusion is<sup>11</sup>

$$e_{ij} = -\frac{P_i}{4} \frac{a^3}{r^3} \left( \frac{3x_i x_j}{r^2} - \delta_{ij} \right).$$

Comparison with Eq. (4) reveals a similar  $1/r^3$  dependence.

(b) Another source of internal strain occurs from material cold working. Plastic flow is believed to occur in local regions, viz., dislocation slip bands.

This leaves elastic strain locked into the material in other regions. A clear example of this occurs in surface working of cylindrical bars leaving a state of hoop stress in the region below the surface. Approximate this state of stress by a uniform pressure  $P$  and again image a spherical inclusion, of compressibility  $K'_T$ , in a medium of compressibility  $K_T$  and shear modulus  $\mu$ . The strain field is

$$e_{ij} = -\frac{1}{3} K'_T P \delta_{ij} + \frac{1}{3} \frac{K'_T - K_T}{1 + \frac{4}{3} \mu K'_T} P \frac{a^3}{r^3} \left( \frac{3x_i x_j}{r^2} - \delta_{ij} \right).$$

Equation (4) for a spherical pore is a limiting case of this solution. On a smaller scale the strain field about point defects is expected to have a  $1/r^3$  dependence. Although the strain field about a line dislocation does not have a  $1/r^3$  dependence, the strain field about a dislocation loop does.<sup>13</sup> In most cases the dominant contributors to internal strain are probably the macroscopic defects such as cavities or inclusions.

This discussion is intended to suggest that in many cases considerable internal strain exhibits a  $1/r^3$  dependence about the source defect. If this is true, then results of this calculation qualitatively apply to material containing residual internal strain.

This conclusion serves to explain several observations regarding the approach to saturation which have not been understood.

(i) It has been observed that, in Eq. (1), the quadratic term  $b/H^2$  is dominant for extremely high magnetic fields, while the linear term  $a/H$  is dominant in intermediate fields.<sup>14</sup> Figure 2 shows that whether a local internal strain region contri-

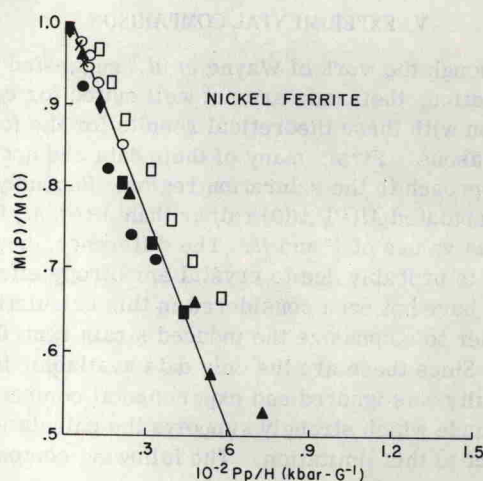


FIG. 6. Magnetization for 0.054 porosity (solid points) and 0.041 porosity (open points) nickel ferrite. The pressure variation is from 2 to 25 kbar.  $\blacktriangle$ ,  $\blacksquare$ ,  $\bullet$ ,  $\blacklozenge$ , and  $\times$  correspond to external applied fields of 45, 100, 325, 980, and 1960 Oe, respectively.  $\square$  and  $\circ$  correspond to 100 and 350 Oe, respectively.